Muon-Spin Rotation Measurements of an Unusual Vortex-Glass Phase in the Layered Superconductor $Bi_{2.15}Sr_{1.85}CaCu_2O_{8+\delta}$

D. O. G. Heron,[1] S. J. Ray,[1] S. J. Lister,[1] C. M. Aegerter,[2] H. Keller,[2] P. H. Kes,[3] G. I. Menon,[4,5,6] and S. L. Lee[1]

[1]*School of Physics and Astronomy, University of St. Andrews, Fife KY16 9SS, United Kingdom*
[2]*Physik-Institut der Universität Zürich, CH-8057 Zürich, Switzerland*
[3]*Kamerlingh Onnes Laboratorium, Leiden University, P. O. Box 9506, 2300 RA Leiden, Netherlands*
[4]*The Institute of Mathematical Sciences, C.I.T. Campus, Taramani, Chennai 600 113, India*
[5]*Mechanobiology Institute, National University of Singapore, T-Lab, No. 10-01 5A Engineering Drive 1, Singapore 117411, Singapore*
[6]*Department of Biological Sciences, National University of Singapore, 14 Science Drive 4, Singapore 117543, Singapore*

Muon-spin rotation measurements, performed on the mixed state of the classic anisotropic superconductor $Bi_{2.15}Sr_{1.85}CaCu_2O_{8+\delta}$, obtain quantities directly related to two- and three-body correlations of vortices in space. A novel phase diagram emerges from such local probe measurements of the bulk, revealing an unusual glassy state at intermediate fields which appears to freeze continuously from the equilibrium vortex liquid but differs both from the lattice and the conventional high-field vortex glass state in its structure.

Magnetic fields penetrate the bulk of a type-II superconductor in the form of quantized vortex lines, which can exhibit several phases [1–3]. Among the most studied of these superconductors is the classic anisotropic superconductor $Bi_{2.15}Sr_{1.85}CaCu_2O_{8+\delta}$ (Bi2212), whose phases have been extensively described both theoretically [1,2,4,5] and experimentally [6–12]. Vortices in Bi2212 order into a hexagonal lattice at low magnetic fields and temperatures [7]. Upon increasing the temperature, this lattice, technically a Bragg glass, melts via a first-order (FO) transition into a vortex liquid phase [8]. A transition also occurs with increasing field at fixed low temperature, to a phase widely believed to be a solid phase with short-ranged order [10,11], in the presence of random pinning [2]. Such a phase can thus be described as a "vortex glass." The transitions from the lattice state to both the liquid and to the short-range ordered solid in Bi2212 have been theoretically [1,2,4] and experimentally [8,10,11] argued to be FO.

Consensus phase diagrams for Bi2212 and related materials rely largely on results from bulk measurements, such as magnetization, which cannot access subtle differences in ordering and structure. Muon-spin rotation (μSR) measurements, which measure the local field distributions of the vortex system in the bulk of the material in order to probe local spatial correlations, were among the first experiments to observe a local microscopic rearrangement of vortices with increasing temperature and field [6,12–14]. Only recently, however, has an adequate theoretical framework been developed to interpret such experiments [12]. In this Letter, we present μSR measurements on Bi2212, using quantities directly related to two- and three-body spatial correlations of vortices to construct a novel magnetic phase diagram for this material. Our studies reveal an unusual glassy state at intermediate fields which appears to

freeze continuously from the equilibrium vortex liquid but differs significantly both from the lattice and the conventional high-field vortex glass state in its local structure. The existence of this glassy state, which we argue should be especially sensitive to perturbations, reconciles a number of prior observations and simulation results for pancake vortices in this field and temperature regime.

In a μSR experiment a beam of spin-polarized muons rapidly thermalizes inside the sample, typically penetrating to a depth of ~ 100 μm [14], thus making μSR a bulk probe of the system. An external field applied perpendicular to the muon-spin polarization causes them to precess at an angular frequency $\omega = -\gamma_\mu B$, where γ_μ is the gyromagnetic ratio of the muon and B is the local magnetic induction at the muon site. The muons decay with an average lifetime of $\tau = 2.2$ μs, emitting positrons preferentially along the muon-spin direction [14], thereby allowing the time evolution of the muon-spin polarization to be measured. The probability distribution of fields experienced by the muons inside the sample, $p(B)$, is obtained from the Fourier transform of the time evolution of the muon-spin polarization $p^+(t)$. The muons are distributed randomly relative to the flux vortices. The spatial modulation of internal magnetic flux density due to the presence of these vortices produces $p(B)$ determined by the spatial correlations of the vortices [6,14–16]. For periodic vortex correlations, subject to small amounts of disorder, there exist a number of analytic models to adequately describe the data in either the time or frequency domain [17]. For nontrivial correlations, Monte Carlo or other numerical approaches may be used to model the detailed shape of $p(B)$ [3,12,18].

In these experiments the field was directed perpendicular to the *ab* planes of a mosaic of the *c* axis aligned

optimally doped Bi2212 crystals with a $T_c = 92$ K. All line shapes were measured after cooling in the applied field from above T_c down to 1.6 K, followed by warming the sample to the measurement temperature. The applied field was never changed below T_c. A smaller subset of data were also measured on a single slightly overdoped single crystal of Bi2212 with a $T_c = 84$ K. All measurements were performed using the GPS spectrometer on the πM3 beam line at the Paul Scherrer Institute in Switzerland, with an experimental arrangement the same as that described in Ref. [12]. The Fourier transformation of $p^+(t)$ was carried out using a maximum entropy method described in Ref. [19].

Each muon line shape $p(B)$ is characterized by a line-width $\sigma = \langle \Delta B^2 \rangle^{1/2}$ and a dimensionless skewness parameter $\alpha = \langle \Delta B^3 \rangle^{1/3} / \langle \Delta B^2 \rangle^{1/2}$, where $\langle \Delta B^2 \rangle$ and $\langle \Delta B^3 \rangle$ are the second and third moments of $p(B)$ and the nth moment has the usual definition $\langle \Delta B^n \rangle = \sum_i p(B_i)(B_i - \langle B \rangle)^n / \sum_i p(B_i)$. Second and third moments $\langle \Delta B^2 \rangle$ and $\langle \Delta B^3 \rangle$ of the field distribution $p(B)$ associated with arrangements of pancake vortices are obtained from

$$\langle \Delta B^2 \rangle = \frac{\rho_\ell}{d} \left(\frac{1}{2\pi} \right)^3 \int d^2 k_\perp \int dk_z S(k_\perp, k_z) |b_z(k_\perp, k_z)|^2$$

$$\langle \Delta B^3 \rangle = \frac{\rho_\ell}{d} \left(\frac{1}{2\pi} \right)^6 \int d^2 \mathbf{k}_{\perp 1} \int dk_{z1} \int d^2 \mathbf{k}_{\perp 2} \int dk_{z2}$$
$$\times S^3(\mathbf{k}_1, \mathbf{k}_2) b_z(\mathbf{k}_1) b_z(\mathbf{k}_2) b_z(|\mathbf{k}_1 - \mathbf{k}_2|), \quad (1)$$

where the field of an individual vortex is given by $b_z = d\Phi_0/(1 + \lambda^2 k_\perp^2 + \lambda^2 k_z^2)$, with d the interlayer spacing, ϕ_0 the flux quantum and λ the penetration depth, and $S(k_\perp, k_z)$ and $S^3(\mathbf{k}_1, \mathbf{k}_2)$ are the pair and triplet structure factor,

respectively [20]. The density $\rho_\ell = B/\Phi_0$. The parameters σ and α are thus related to averages over the local two-body and three-body correlations of the vortex state [12,15].

Figures 1(a)–1(d) show four distinct μSR line shapes measuring the probability distributions $p(B)$ of the internal magnetic fields of the superconductor at different applied fields and temperatures, obtained after cooling from above T_c in an applied field. The characteristic line shape for a vortex-line lattice, represented by the data of Fig. 1(a), is well understood [6,12,15]. It is marked by an $\alpha > 0$ arising from a higher spectral weight at fields greater than the mean. This changes to a $p(B)$ with an $\alpha < 0$ [Fig. 1(b)] at the FO melting line [6,12,13] [see also Fig. 1(e)]. It has been shown theoretically that negative third moments have a subtle origin, requiring nontrivial three body correlations in addition to a structure factor $S(q)$ that is broadened in comparison to the Bragg peaks associated with a crystalline phase [12], as would be expected in a phase with short-ranged order [12]. In the remainder of this Letter we focus on the vortex configurations that lie outside of these low-field lattice and liquid phases, where much less is understood about the nature of local vortex correlations.

An additional change with temperature from an $\alpha > 0$ [Fig. 1(d)] to an $\alpha < 0$ [Fig. 1(b)] state occurs at high field [Fig. 1(f)]. The corresponding states are designated as region 3 and region 4, respectively, in the phase diagram of Fig. 2. The high-field low-temperature phase (region 3) is distinguished from the vortex lattice phase (region 1) by much reduced values of the linewidth σ and α. This *reduction* of σ at low temperature can only occur if off-layer vortex correlations are substantially reduced
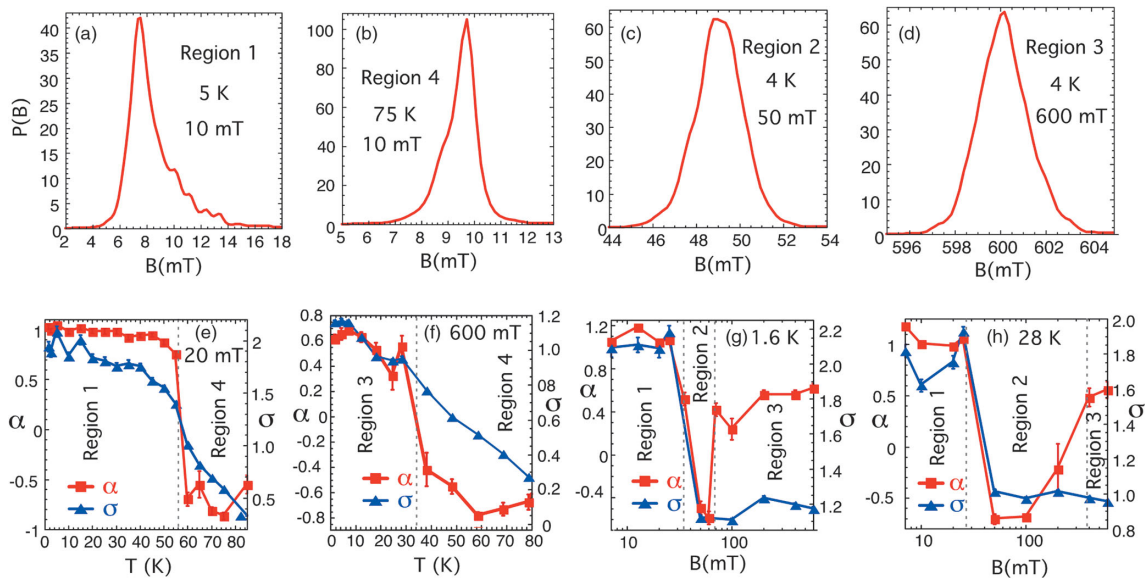

FIG. 1 (color). (a)–(d) Representative muon line shapes $p(B)$ from different regions of the phase diagram at (a) 10 mT, 5 K [region I of Fig. 2(a)]. (b) 10 mT, 75 K (region 4). (c) 4 K, 50 mT (region 2). (d) 4 K, 600 mT (region 3). (e) The evolution with temperature of α and σ (see text) across the melting line at $B = 20$ mT. (f) Changes of α and σ at the glass-liquid boundary ($B = 600$ mT). (g), (h) The evolution with field of α and σ (at $T = 1.6$ and $T = 28$ K, respectively) For all measurements the samples were first cooled in an applied field from above T_c to 1.6 K.

[6,13–16]. These features are well-captured by analytic calculations (see Supplemental Material [21]) which use liquid state and density functional methods together with known material parameters to describe vortices in Bi2212, assuming that vortex correlations in this glassy state resemble those in a correlated fluid of two-dimensional pancake vortices (Supplemental Material [21]). This glass phase is characterized not only by short-ranged correlations perpendicular to the conduction planes but also by nontrivial correlations *within the planes*, leading to a positive α. In our calculational framework, the in-plane structure factor in the vicinity of its first peak $S(q_\perp \sim 2\pi/a, q_z)$ is broadened by thermal fluctuations as temperature is increased, reducing α from an initial positive value till it eventually becomes negative (Supplemental Material [21]). This differs significantly from previously reported behavior in the high-field glassy states formed from line vortices in the far less anisotropic material $La_{1.9}Sr_{0.1}CuO_4$ [12], where off-layer correlations are strong enough that vortices retain their identity as lines rather than pancakes. Although, in Bi2212, α exhibits a rapid change of sign with temperature [Fig. 1(f)], it is not obvious that this necessarily reflects a thermodynamic transition, since in the analytic calculations, such a change can be obtained as $S_\perp(q)$ is continuously broadened. The experimental data, however, further exhibit a change of slope of σ at this boundary [Fig. 1(f)], suggesting a rapid rate of change of $S(q)$ possibly reflecting collective behaviour in the vicinity of the macroscopic irreversibility line (IL). Such a reduction in σ can arise, for example, due to rapid thermal fluctuations of wave vector $\mathbf{q} = (\mathbf{q}_\perp, q_z)$ ("motional narrowing") or from slow fluctuations of wave vector q_z [15,16]. We also note that a value of $\alpha < 0$ is a characteristic of all measurements made above the macroscopic IL in the liquid state [Fig. 2(a)].

Our most intriguing finding concerns the vortex arrangement at *intermediate* fields, between the lattice and the glass phases [region 2 of Figs. 2(a) and 2(b)]. A line shape typical of this intermediate field regime is shown in Fig. 1(c). In common with the high-field glass state (region 3) it has a substantially reduced value of σ compared to the lattice phase, indicating that the pancake vortices no longer form the well-ordered lines found in the latter. Moreover, it shares several common features with line shapes in the liquid phase [Fig. 1(b)], most significantly, $\alpha < 0$, in contrast to region 3 [12]. The transitions with fields into and out of this region 3 are most clearly seen in Figs. 1(g) and 1(h), summarized in Fig. 2. While region 2 is clearly distinguished in line shape (and therefore α values) both from the lattice and the high-field glass phase, it is less obviously differentiated from the liquid state found at higher temperature. Bulk measurements, however, show strongly irreversible behavior below the IL implying that vortices are not free to flow. Given the apparent continuity to the liquid state, one interpretation of this region is of a lagoon of pinned liquid: that is, a region having spatial correlations close to those in the liquid state but where the bulk motion
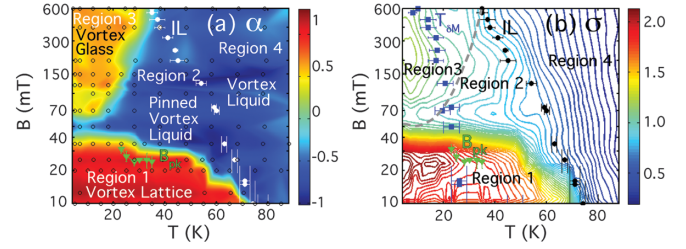

FIG. 2 (color). The variations across the *H-T* plane of (a) α and (b) σ (in mT). Region 1: $\alpha > 0$, high σ (vortex lattice). Region 2: $\alpha < 0$, low σ. Lines soften into a glassy arrangement of pancake vortices, but correlations retain a liquidlike character (see text). Region 3: $\alpha > 0$, low σ. Glass of pancake vortices. Region 4: $\alpha < 0$, low σ. Above the macroscopic IL in the liquid state. The plotted points are closed white or black circles: the IL (from bulk magnetization), green triangles: the second peak B_{pk} in the magnetization $M(B)$, blue squares: the peak in the gradient with temperature $T_{\delta M}$ of the zero field-cooled magnetization, open black circles: the coordinates of μSR data points. The bulk IL is closely connected to the contours of σ, above which the gradient increases.

of vortices is strongly inhibited by the pinning landscape. We cannot rule out, however, the possibility that more exotic alternatives, such as a "slush" of fluctuating liquid and solid domains with a specific distribution of domain sizes, might yield similar structural attributes. Evidence that this state is distinct from the liquid state in terms of *local* behavior comes from a further subtle signature of the bulk IL found in this region, reflected in the variation of $\sigma(B, T)$ at the IL [Fig. 2(b)]. While the value of $\sigma(T) \propto b^{-1}(\mathbf{q}) \propto \lambda_{ab}^{-2}(T)$ [Eq. (1)] and hence is expected to fall smoothly as T approaches T_c, there are additional more rapid local variations in the *gradient* $\nabla_{B,T}(\sigma)$ at the IL, most evident in the contour plot of σ [Fig. 2(b)]. The existence of the lagoon at lower fields is thus manifest in $\sigma(B, T)$ as a triangular region of gently sloping contours [Fig. 2(b)] that become more closely spaced above the IL. As discussed above, this is consistent with the onset of additional motional narrowing above the IL where dynamics increase.

The nature of the vortex state in the region that surrounds the vortex lattice phase has long been the source of much experimental [6–12] and theoretical debate [1–3,5,10,11,18]. This region has proved notoriously difficult to equilibrate *via* numerical simulations [5,22,23]. By contrast, the glass and lattice phases at higher and lower field are clearly seen in the simulations. In our own calculations, the simplest model which assumes that fluid structure is simply frozen in, in the vicinity of the irreversibility line (see Supplemental Material [21]), also fails to capture the unusual behavior in region 2, in particular the increase in temperature with field of the line separating $\alpha > 0$ from $\alpha < 0$. Within such models, the temperature at which α changes from positive to negative always increases with decreasing field, qualitatively following the slope of the flux-lattice melting phase boundary. This is opposite to the situation observed experimentally between region 3 and
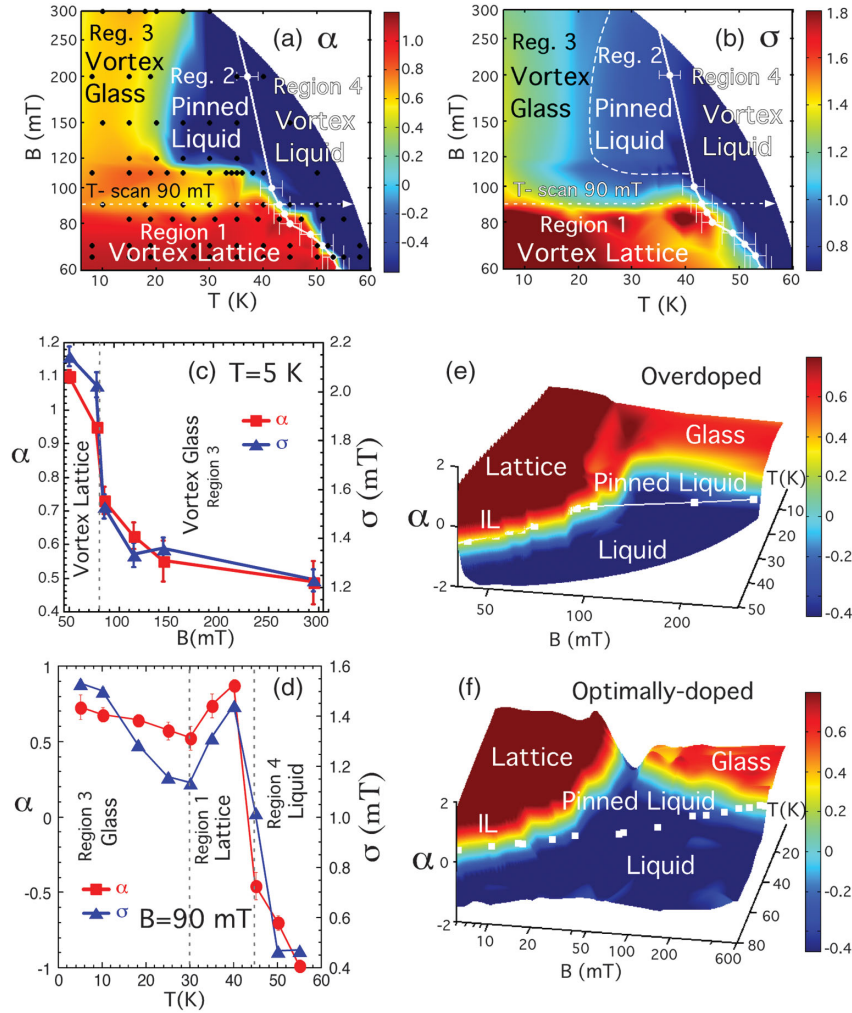
FIG. 3 (color).   The variations across the H-T plane of (a) α and (b) σ (in mT) for an *overdoped* sample of Bi2212, showing the peak in the FO vortex lattice phase boundary reported in thermodynamic measurements of similar samples [8–11]. Filled black circles are the coordinates of μSR data points. (c) The change with field of α and σ at 5 K, *without* the change to $\alpha < 0$ observed in the optimally doped system [Figs. 1(g) and 1(h)]. (d) The variation of α and σ along the line of constant $B = 90$ mT shown in (a) and (b), described in Ref. [10] as the inverse melting to a vortex lattice with temperature. (e)–(f) Comparison for the overdoped and optimally doped samples of α around the "lagoon" of the novel $\alpha < 0$ pinned liquid state (white circles are the IL). In the overdoped system the vortex lattice phase directly adjoins the highly disordered glassy phase. The pinned liquid now forms a vestigial triangular region adjacent to the liquid phase. In the vicinity of the FO phase line the origin of the inverse melting process can now be understood [10].

region 2. Thus, simply freezing in correlations at the IL cannot replicate the observed behavior in region 2.

To understand this unusual phase, we propose that thermal and disorder-induced fluctuations are *qualitatively* more important in the low field glassy state (region 2) as opposed to the high field vortex glass (region 3), allowing the vortex system access to a significant number of nearly equivalent free-energy minima. Since this regime is strongly irreversible, these fluctuations most likely result in strong local positional fluctuations ("rattling") about a quenched *fluid structure*, rather than the large-scale shifts of vortex structure which can occur in a liquid which can flow. Parametrizations of the structure factor which account for such fluctuations within the glassy state predict that the change of sign is shifted towards lower temperatures for a given applied field, yielding a lagoon in which α

remains negative, as in the experiments (Supplemental Material [21]). Although this strong additional assumption is required *ad hoc* to model the data, it is consistent with previous experimental studies suggesting an enhanced role for thermal fluctuations in such a glassy state [11,24–26], including evidence for a depinning line well below the IL [25,26], as well as the simulations which found it hard to equilibrate in this regime. The discontinuous onset of both the high field glassy regime (region 3), when increasing the field from region 2 [Fig. 1(g)], or the lattice state when decreasing the field from region 2, strongly suggests that the *pinned liquid lagoon* is a new glassy state of vortex matter, distinct from the vortex glass.

Previous careful magnetization experiments on slightly overdoped (less anisotropic) samples of Bi2212 showed no signs of the novel pinned liquid state reported here [8–11],

reporting instead a FO line from the vortex state with a peak in temperature at around 35 K, bounded at low temperature by the vortex glass and at higher temperatures by the vortex liquid. This is the unusual phenomena of "inverse melting" [10], whereby an amorphous phase transforms, with increasing temperature, to a crystalline phase of higher entropy, stabilized by enhanced *thermal* fluctuations in the crystalline phase. It has been reported that this peak in the FO line of Bi2212 is found only in overdoped samples and not in underdoped or optimally doped systems [9]. To elucidate these differences we performed muon experiments on overdoped crystals of Bi2212 similar to Refs. [9,11] (Fig. 3). For these data both α and σ contain signatures (Fig. 3) of the peak in the FO line previously reported in Ref. [10]. We note that these occur in our system at higher field, attributable to differences in stoichiometry, which strongly affects the *position* of the peaked line in the overdoped region [9–11]. Interestingly, the glass (region 3) and the lattice (region 1) are, in this case, no longer separated by the $\alpha < 0$ pinned liquid region found in the optimally doped system. There is thus a *direct transition* with field from a lattice to a glass phase, measured to be FO in Refs. [10,11]. By scanning in temperature through the peak at 90 mT a nonmonotonic dependence of both α and σ is observed (Fig. 3(d)). At 90 mT and 5 K the system is just inside the glass state [Fig. 3(c)]. On increasing the temperature both α and σ both fall initially [Fig. 3(d)], indicating greater disorder, where upon both increase again above around 30 K. The increase of σ is consistent with enhanced c-axis correlations as the temperature is increased, likely arising from increased thermal mobility allowing vortices to recover partial alignment along the c direction over a narrow region of temperature. At higher temperatures, the lattice melts.

In conclusion, we have reexamined the phase diagram of a prototype vortex matter system using local probe measurements. The phase boundaries previously inferred from theoretical and experimental studies are clearly apparent in variations in the moments of the field distribution. We identify an additional lagoon of novel pinned liquid below the IL, especially prominent in the optimally doped system, with spatial correlations very similar to those in a vortex liquid phase, but enhanced thermal and disorder-induced fluctuations in comparison to the high-field vortex glass state. Significantly, several features of bulk measurement techniques, including the IL and the FO melting line of the lattice, are mirrored in the contours of the second moment of the field distribution. Thus, they can be linked to variations in two-body correlations in the vortex system, a connection which may be useful in delineating glassy phases which differ in subtle ways. These results should stimulate further theoretical work on this generic phase diagram, in addition to providing a useful framework for the interpretation of experimental work on bulk properties of anisotropic superconductors. More generally, our elucidation of a novel glassy state of vortices, with a heightened sensitivity to thermal and disorder-induced fluctuations, provides a better understanding of why past work found such states difficult to equilibrate, while suggesting a new experimental system to explore the physics of disorder-induced glassy states, including the complex free-energy landscape known to be a characteristic feature of glassy systems.

[1] G. Blatter, M. V. Feigel'man, V. B. Geshkenbein, A. I. Larkin, and V. M. Vinokur, Rev. Mod. Phys. **66**, 1125 (1994).

[2] T. Giamarchi and P. Le Doussal, Phys. Rev. B **52**, 1242 (1995).

[3] G. I. Menon, Phys. Rev. B **65**, 104527 (2002).

[4] S. Sengupta, C. Dasgupta, H. R. Krishnamurthy, G. I. Menon, and T. V. Ramakrishnan, Phys. Rev. Lett. **67**, 3444 (1991).

[5] P. Olsson and S. Teitel, Phys. Rev. B **79**, 214503 (2009).

[6] S. L. Lee *et al.*, Phys. Rev. Lett. **71**, 3862 (1993).

[7] R. Cubitt *et al.*, Nature (London) **365**, 407 (1993).

[8] E. Zeldov, D. Majer, M. Konczykowski, V. B. Geshkenbein, V. M. Vinokur, and H. Shtrikman, Nature (London) **375**, 373 (1995).

[9] B. Khaykovich, E. Zeldov, D. Majer, T. Li, P. H. Kes, and M. Konczykowski, Phys. Rev. Lett. **76**, 2555 (1996).

[10] N. Avraham *et al.*, Nature (London) **411**, 451 (2001).

[11] H. Beidenkopf, N. Avraham, Y. Myasoedov, H. Shtrikman, E. Zeldov, B. Rosenstein, E. H. Brandt, and T. Tamegai, Phys. Rev. Lett. **95**, 257004 (2005).

[12] G. I. Menon *et al.*, Phys. Rev. Lett. **97**, 177004 (2006).

[13] T. Blasius, Ch. Niedermayer, J. Tallon, D. Pooke, A. Golnik, and C. Bernhard, Phys. Rev. Lett. **82**, 4926 (1999).

[14] J. E. Sonier, J. Brewer, and R. Kiefl, Rev. Mod. Phys. **72**, 769 (2000).

[15] E. H. Brandt, Phys. Rev. B **37**, 2349 (1988).

[16] E. H. Brandt, Phys. Rev. Lett. **66**, 3213 (1991).

[17] A. Maisuradze, R. Khasanov, A. Shengelaya, and H. Keller, J. Phys. Condens. Matter **21**, 075701 (2009).

[18] G. I. Menon, C. Dasgupta, and T. V. Ramakrishnan, Phys. Rev. B **60**, 7607 (1999).

[19] T. M. Riseman and E. M. Forgan, Physica (Amsterdam) **289–290B**, 718 (2000).

[20] J. P. Hansen and J. R. McDonald, *Theory of Simple Liquids* (Academic, New York, 2005), 3rd ed.

[21] See Supplemental Material at http://link.aps.org/supplemental/10.1103/PhysRevLett.110.107004 for a detailed description of the numerical methodology mentioned in the text and high-quality versions of Figs. 2(a) and 3(a).

[22] Y. Nonomura and X. Hu, Phys. Rev. Lett. **86**, 5140 (2001).

[23] C. Dasgupta and O. T. Valls, Phys. Rev. B **76**, 184509 (2007).

[24] H. Beidenkopf, T. Verdene, Y. Myasoedov, H. Shtrikman, E. Zeldov, B. Rosenstein, D. Li, and T. Tamegai, Phys. Rev. Lett. **98**, 167004 (2007).

[25] D. T. Fuchs, E. Zeldov, T. Tamegai, S. Ooi, M. Rappaport, and H. Shtrikman, Phys. Rev. Lett. **80**, 4971 (1998).

[26] E. M. Forgan, M. T. Wylie, S. Lloyd, S. L. Lee, and R. Cubitt, Czech. J. Phys. **46**, 1571 (1996).